

Baroclinic Ekman spirals

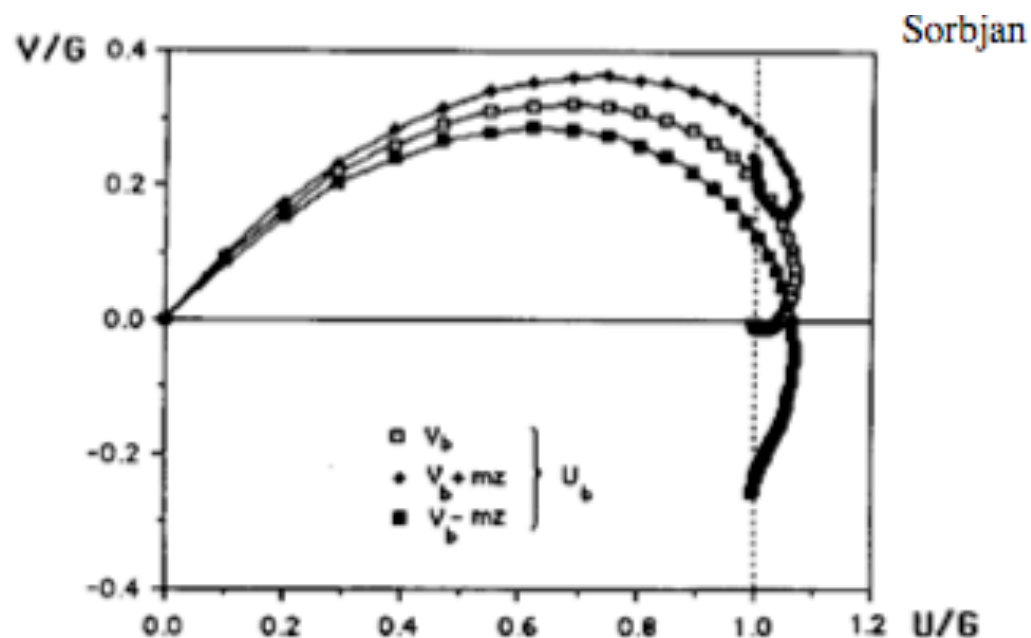
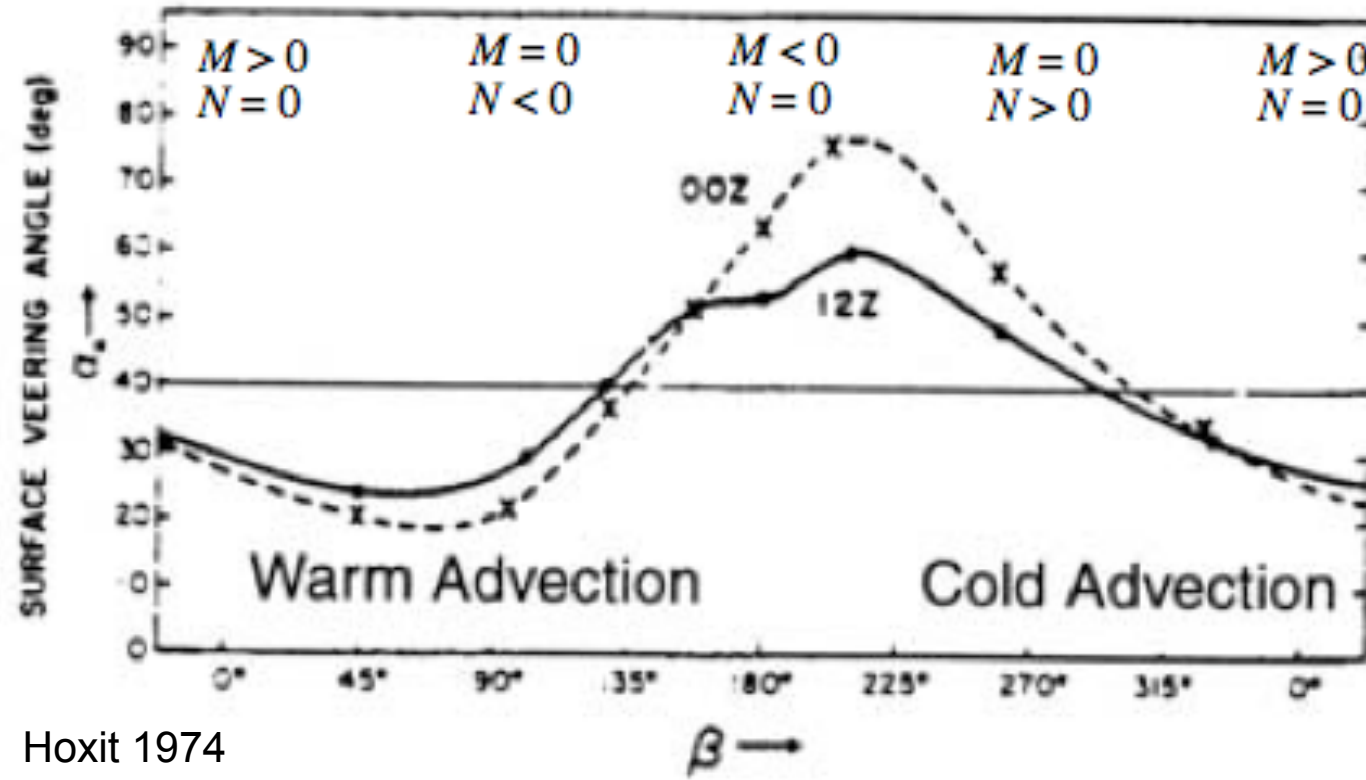
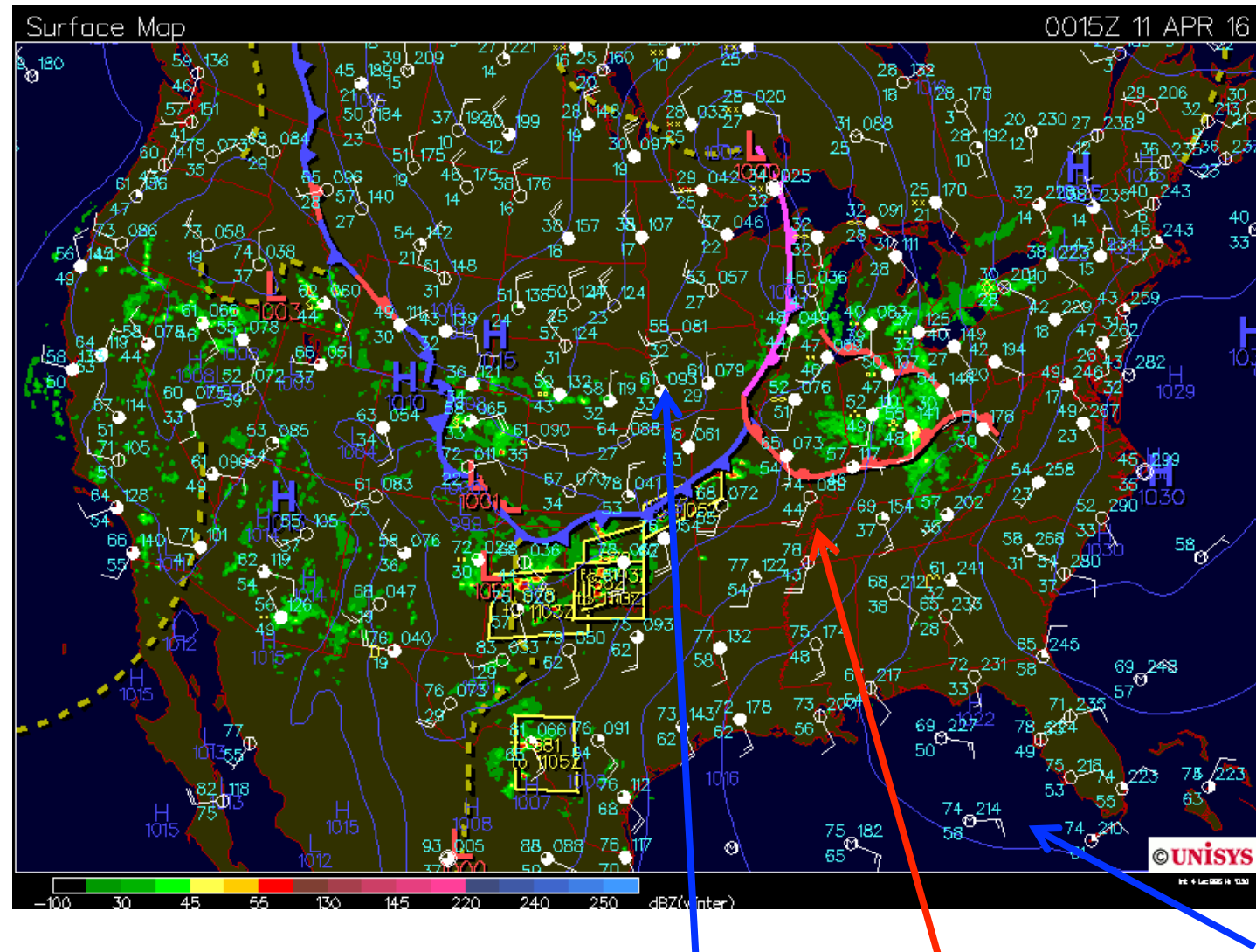


Figure 6.11 Ekman spirals obtained for the baroclinic correction of the V component of the wind velocity, $a = 0.001$, $m = 0.0001$. Points are plotted every 100 m, starting on the surface. U_b , V_b -barotropic components of the wind vector. Dotted line shows directions of the thermal wind vectors.

Surface wind crossing angle vs. thermal wind



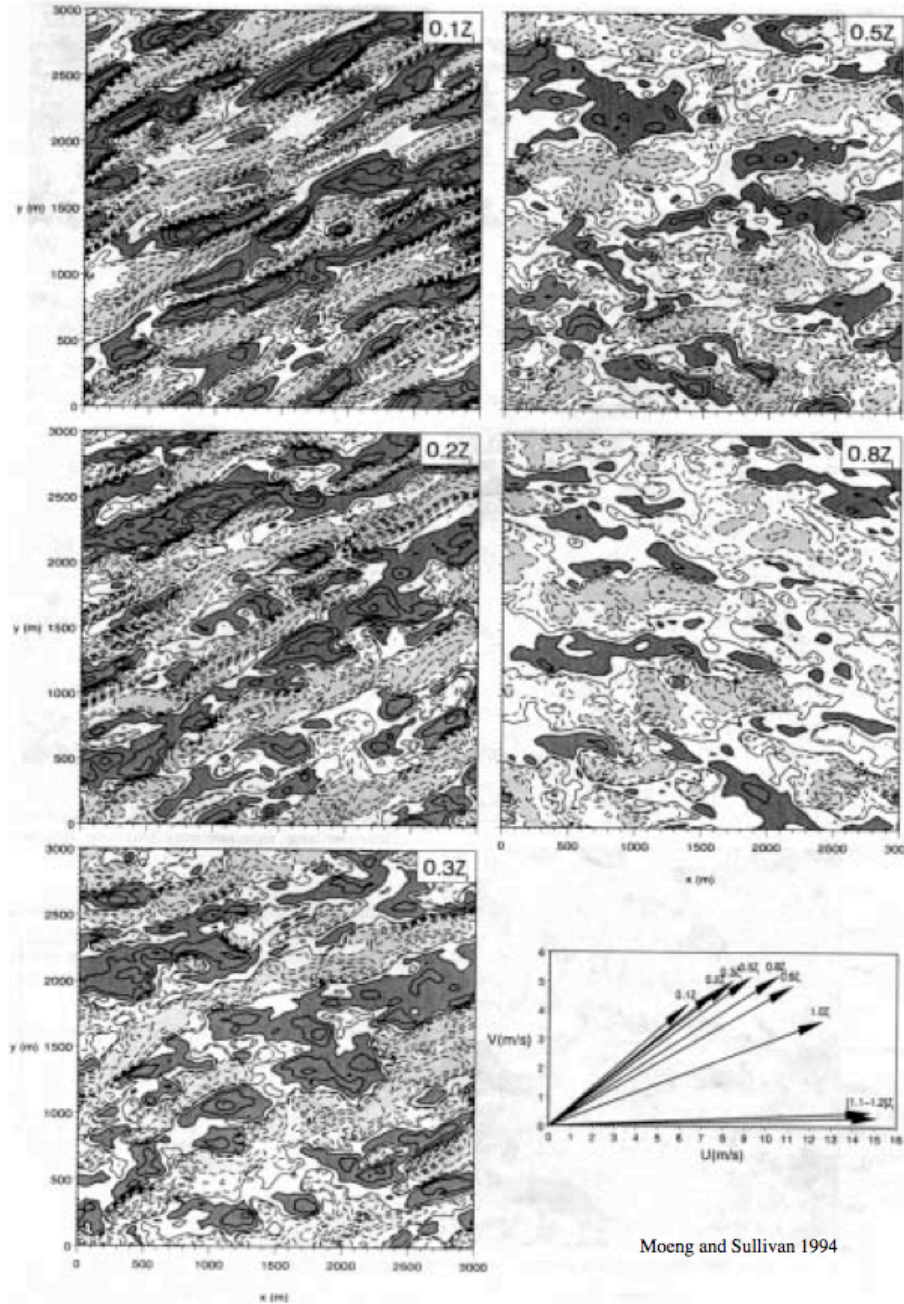


Cold advection:
cross-isobar flow

Warm advection:
Along-isobar flow

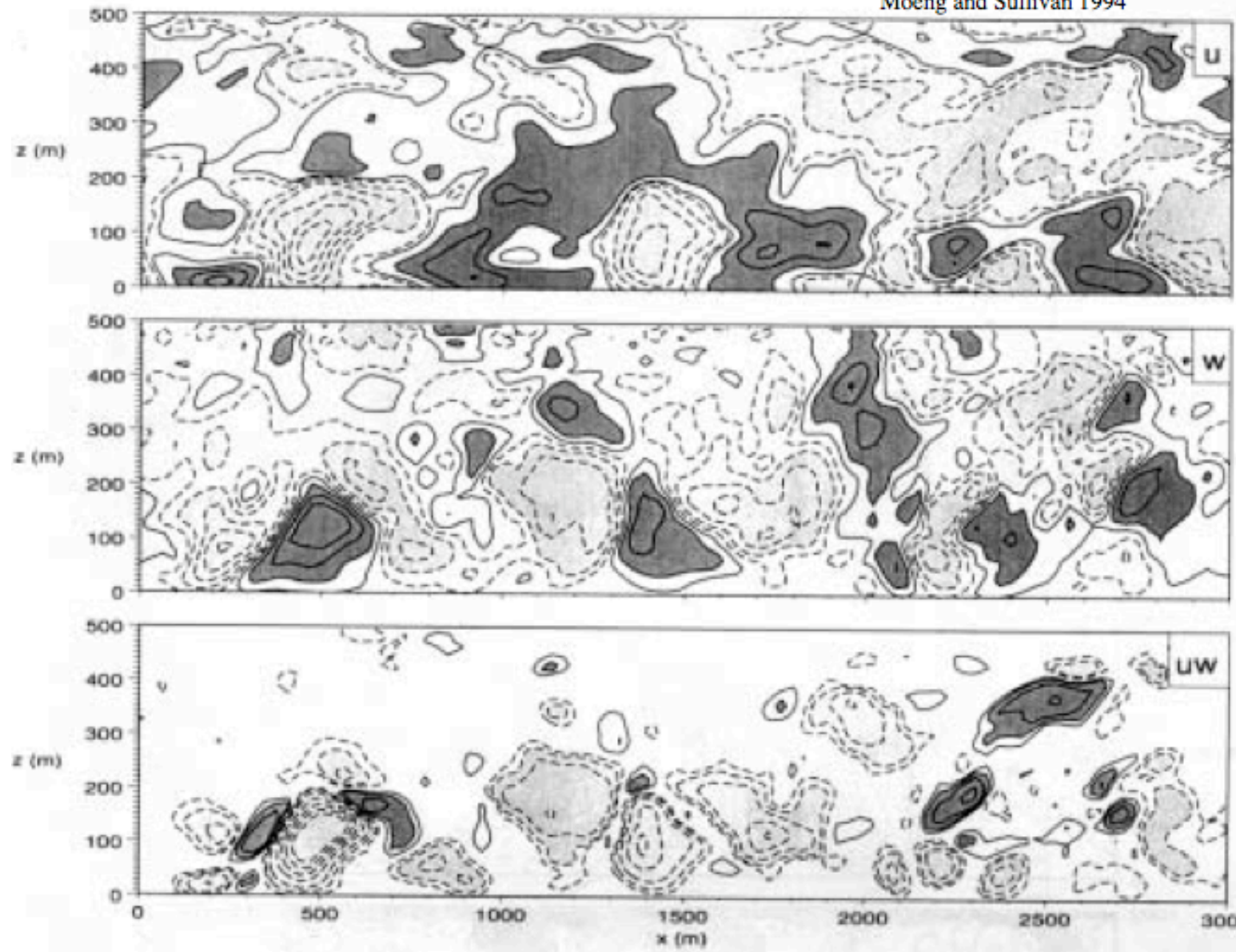
Over water:
along-isobar flow

Horizontal sections of u' from LES of shear-driven turbulence

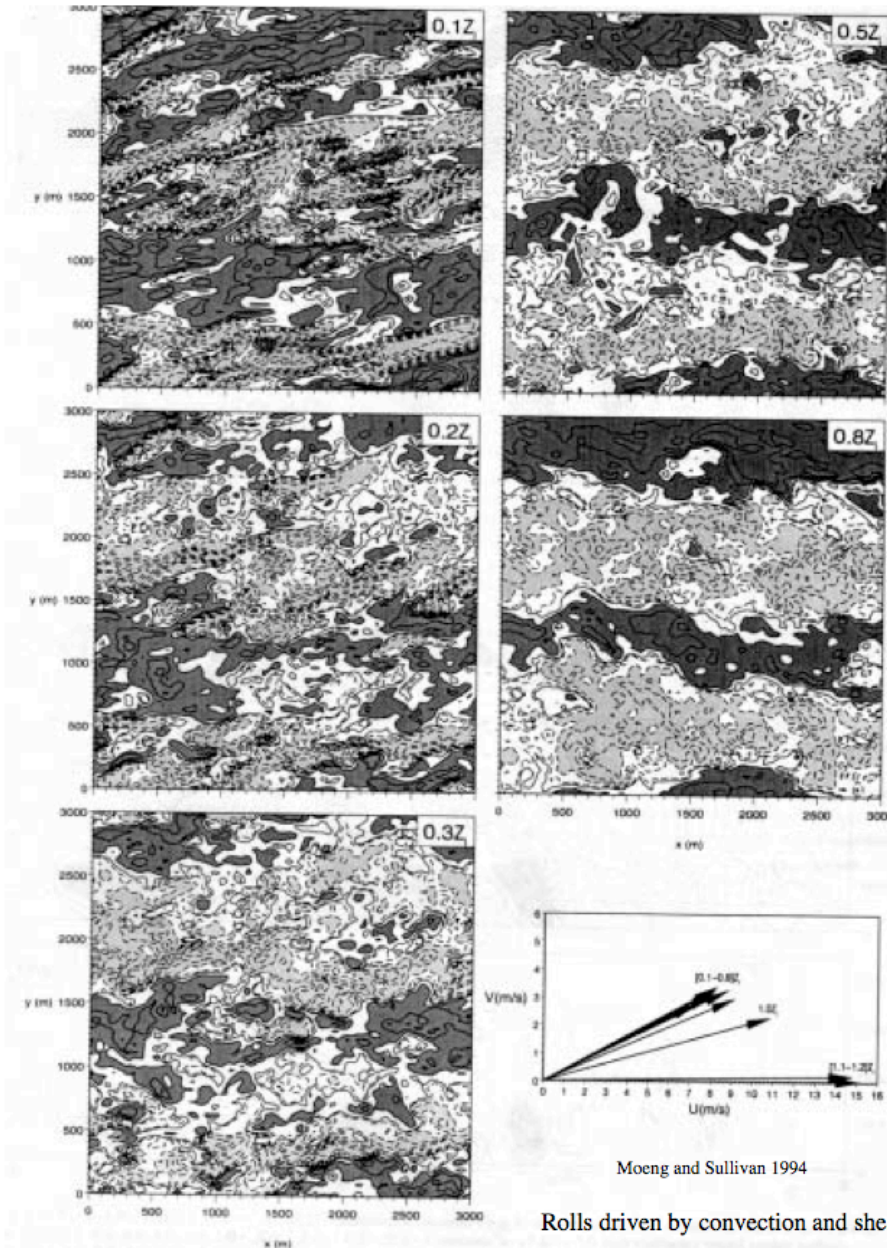


LES vertical section of u' in shear-driven PBL

Moeng and Sullivan 1994



Rolls in LES weakly convective PBL

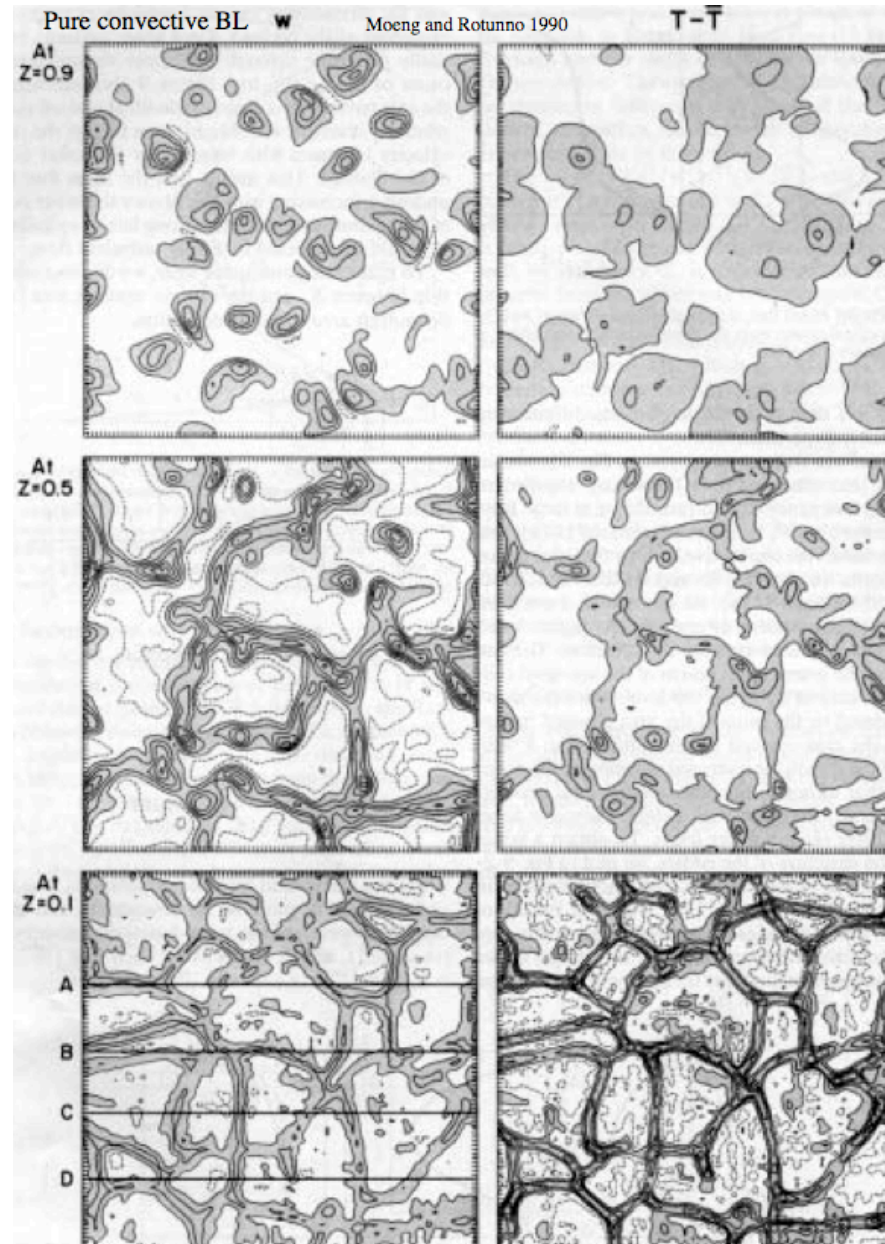


Moeng and Sullivan 1994

Rolls driven by convection and shear.

FIG. 15. Views of $x-y$ for simulation SB1 for u field at five height levels and its wind hodograph: contours ($-3, -2.5, -2, -1.5, -1, -0.5, -0.1, 0.1, 0.5, 1, 1.5, 2$), dark (light) shading values larger (smaller) than 0.5 (-0.5). Some height labels in the wind hodograph are grouped since winds at those levels are about the same.

Convective PBL (Rayleigh-Benard)



Velocity variance profiles

Moeng and Sullivan 1994

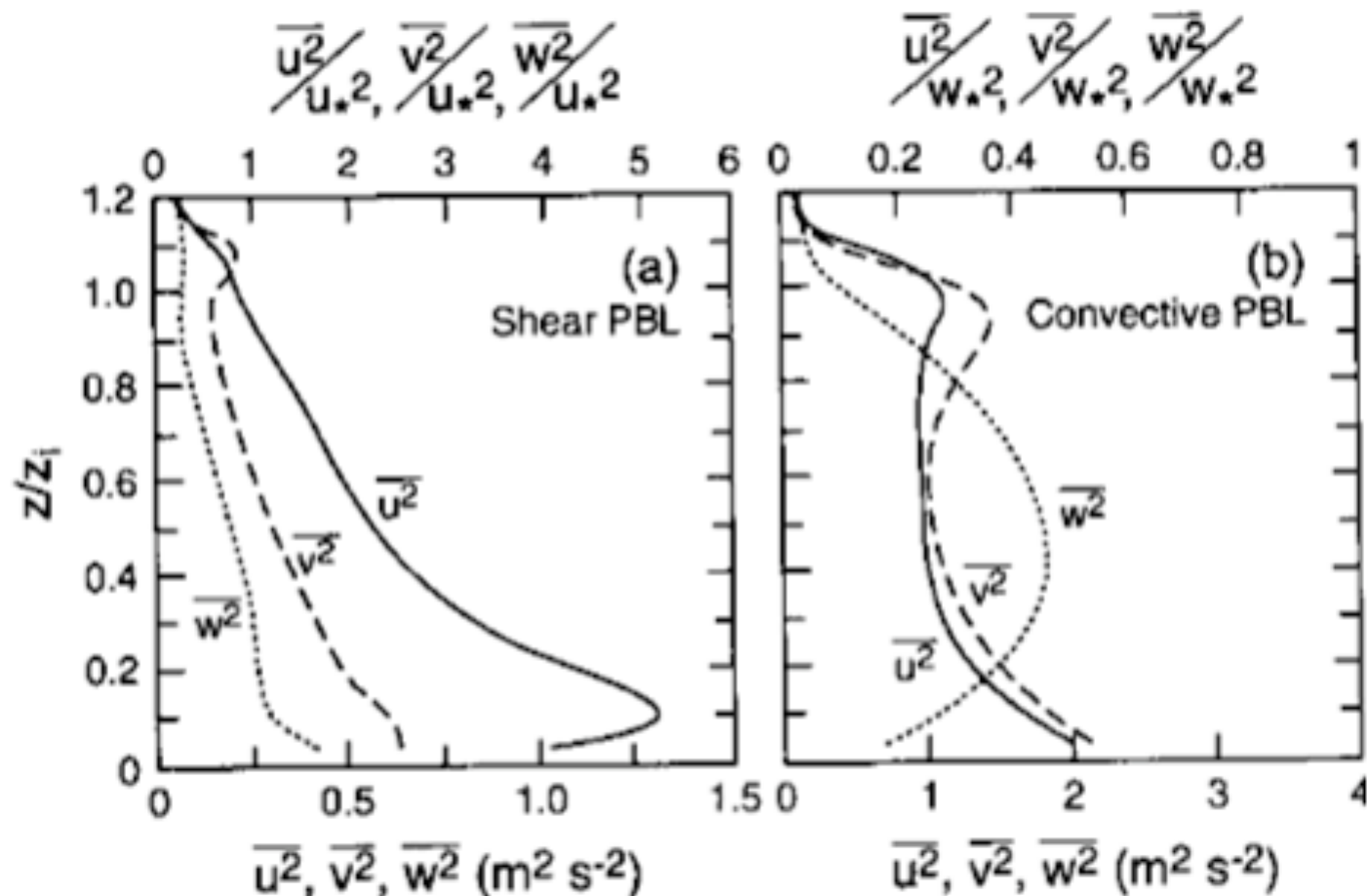


FIG. 9. Vertical distributions of the velocity variances of simulations S and B.

TKE budgets

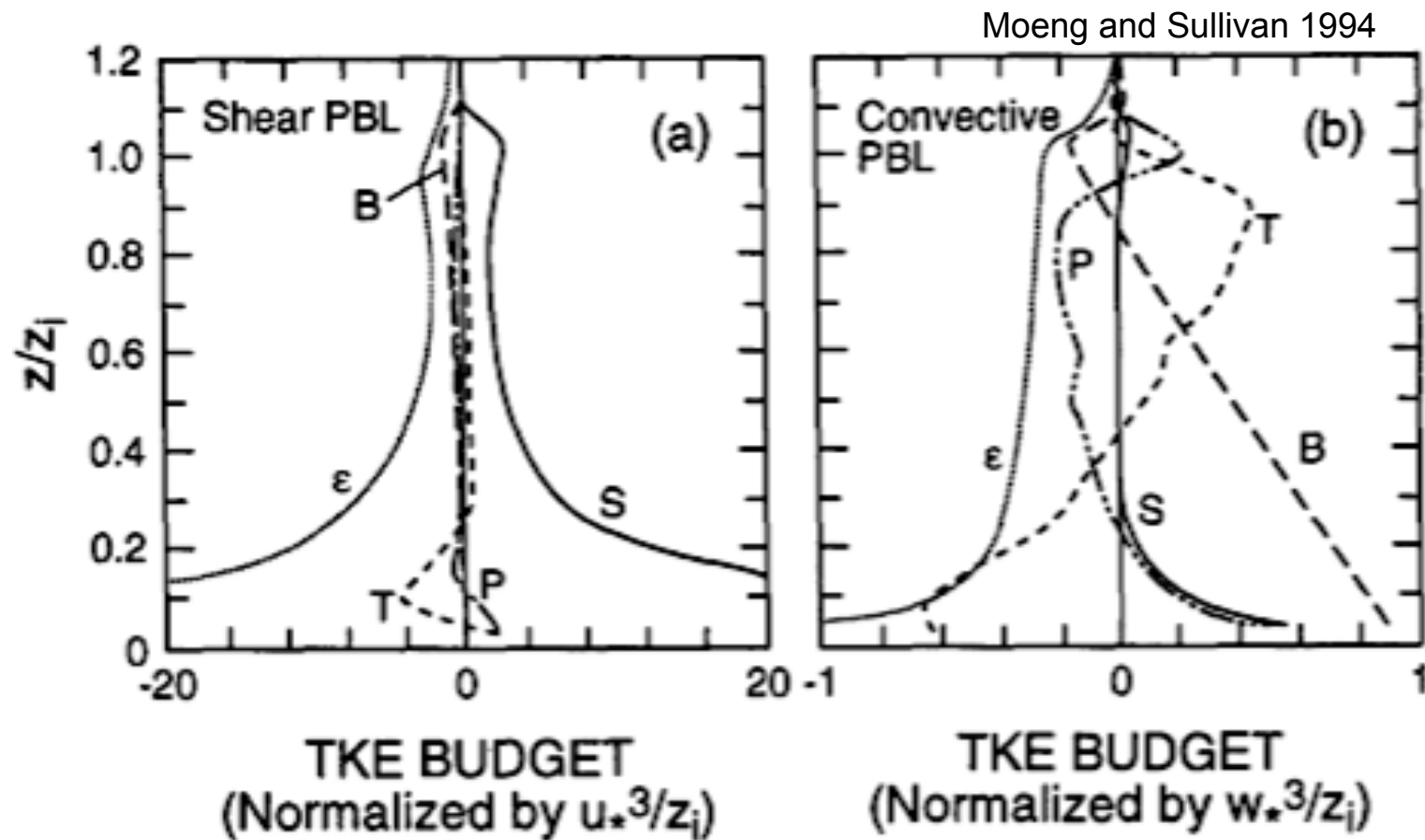
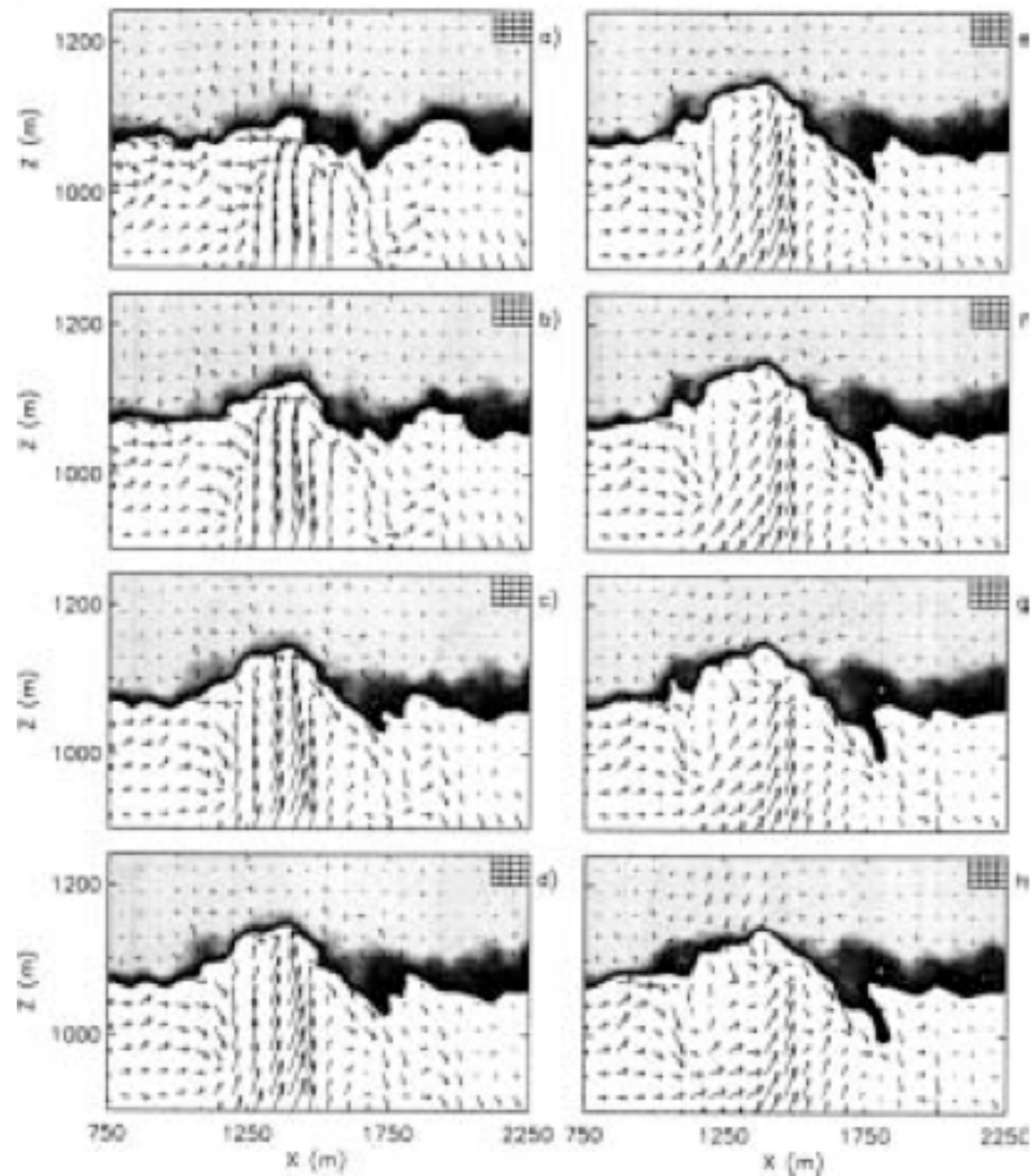


FIG. 11. Vertical distributions of the terms in the TKE budget computed directly from simulations S and B.

LES-simulated entrainment event in a convective PBL



Sullivan et al. 1998

Atm S 547 Lecture 7, Slide 10

Observational support for DCBL entrainment closure

$$\overline{w'b'}(h) = -0.2B_0$$

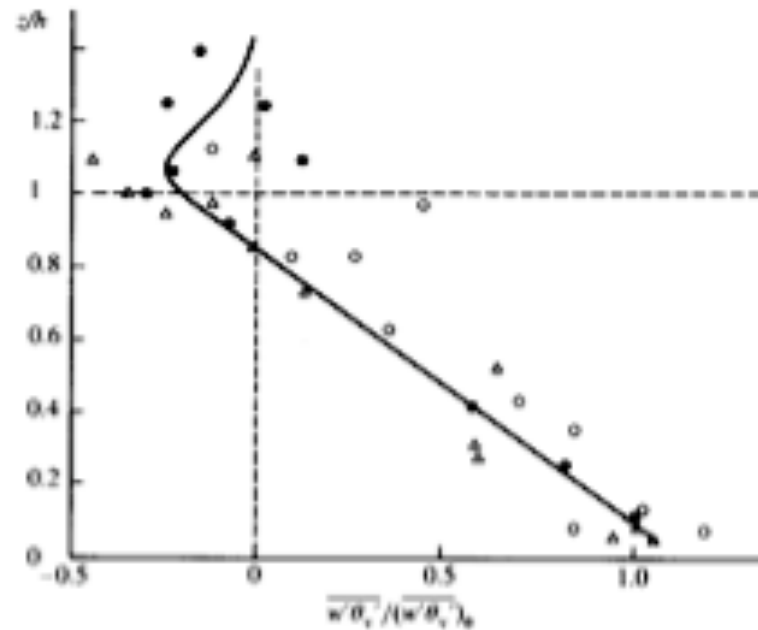


Fig. 6.2 Experimental data on the vertical variation of the virtual heat flux, normalized by its surface value; h is the depth of the mixed layer. Data are for three days from the 1983 ABL experiment; see Stull (1988, Figs. 3.1, 3.2 and 3.3). See also Fig. 6.23 of this volume.